

Responses to reviewers

We thank the reviewers for a careful reading of our manuscript. In this text, we present the answers to the reviewers comments. Also, we are including below the revised version of the manuscript (modifications in red).

Response to Reviewer 1

We thank the reviewer for a careful reading of our manuscript and for listing the mistakes/typos in figure captions etc., which have been corrected in the revised version.

Regarding the additional comments on the scientific part, the reviewer says

“- Relationship in Eq. (1) is a very particular one. The authors identify deviations from it as ‘nonlinearity’. Please note that standard linear relationships such as $y(t)=\int_0^t g(t-t') x(t') dt$ are also linear but different from (1). The authors should comment or state that they are looking at linear relationships involving only the present time and one past time, instead of a more general linear relationship involving a distribution of delays.”

Authors’ response: we agree with the reviewer and in the revised manuscript we have included the following sentence: We note that more generic relations such as $y(t)=\int_0^t g(t-t') x(t') dt$ are also linear, however, here we only consider linear relationships involving only the present and only one past time.

The reviewer says

“- The authors do not state with precision their discretization procedure to define the entropy measure. And the precise form of the discretization is determinant for the entropy values. It is puzzling to read the statement that the presence of outliers ‘decreases entropy’. This is exactly the effect contrary to what one should expect from outliers, since the outliers broaden the distribution. Perhaps the authors are adapting the range of values of SATA to the changing range of extreme values at different positions? Only in this way one could expect some entropy decrease with outliers, but this procedure completely destroys any possibility of inter-site comparison. Since there is no statement of neither the range of discretization nor of bin size (only number of bins is stated) there is no way to check the origin of the reported increase of entropy. For fixed bin size and range across the different locations, appearance of extreme values can only increase entropy.”

Authors’ response: We disagree with the reviewer that “this procedure completely destroys any possibility of inter-site comparison”, on the contrary, we show that in this way the entropy analysis uncovers coherent

spatial structures and identifies localized regions where extreme values (likely to be artefacts) are present in the time-series.

These local extreme fluctuations cannot be detected if a fixed bin size and range are used, to compute the entropy, across all datasets. As we say in the manuscript, each time series is first normalized to zero mean and unit variance, and some fluctuations are extreme with respect to the local statistical distribution of SAT (or SATA) fluctuations.

The reviewer says

- *Page 3: 'this gives approximately the same number of data points per bin': this should apply not to each bin, but to some average value, right?'*

Authors' response: We agree with the reviewer and in the revised manuscript we have replaced approximately by average.

The reviewer says

- *The authors attribute the difference in behavior of the tropical zones to the use of solar radiation in evaporation instead of heating. This sounds reasonable. But one can imagine other possible explanations contributing to this, as for example the smaller amplitude of the variation in solar forcing, or the fact that between the tropics the annual cycle has two oscillations in solar intensity instead of only one. The authors should comment on that. In general, the identification of the physical phenomena that could be responsible for the observations reported in the paper are rather superficial.*

Authors' response: We agree that it may additionally have to do with the fact that these are regions with a small amplitude of the seasonal cycle. On the other hand, the insolation we are using to compare with the SAT response has the semi-annual cycle included and if the response were linear the SAT would also have two peaks and the distance would be small.

In the revised version we have also improved the discussion about the physics responsible for the nonlinear response.

The reviewer says

- *I found difficult to recognize that the different time series in fig 3 correspond to the different locations inside the stated coordinate range. Perhaps this should be explicitly stated.*

Authors' response: We have improved the caption of this figure to clarify the panels.

Response to Reviewer 2

The reviewer says

“An ad-hoc measure for nonlinear relationships between time series is used, ignoring well established measures that are readily available in the literature. The present results should be compared to those obtained from well-established measures such as mutual information.”

Authors' response: The measure we use is a known distance between two time-series and in the revised version we have included a sentence about this point including references. In the Supplementary Information we compare with another distance measure and we obtain similar results (Fig. 2 of the SI). The mutual information is not appropriate because the insolation is a fully deterministic periodic signal.

The reviewer says

“The motivation and aim of the study is not clear: the paper sets of in the introduction with discussing climate networks in the first paragraph. But the rest of the paper does not have anything to do with climate networks.”

Authors' response: We have rewritten the introduction to better motivate this study.

The reviewer says

“The relations-ships between the ad-hoc measure for nonlinear relationships and entropy are discussed only vaguely without supporting statistical analysis. Scatter plots between both quantities would help to support the claims made in the text. Further analysis should follow to substantiate them. What has improved to some degree in my opinion is the discussion of the physical mechanisms possibly underlying the observed patterns.”

Authors' response: In the revised manuscript we include and discuss the scatter plots. We are pleased that the reviewer considers that the discussion has improved with respect to previous version and we hope that the revised version will convince the reviewer that the analysis performed here uncovered meaningful information about our climate.

Response to Reviewer 3

The reviewer says:

"This manuscripts could be helpful for researchers to decide whether to use linear or nonlinear measures when constructing climate networks."

Authors' response: We are pleased that the reviewer appreciates the connection and believes that our work could be helpful for research in climate networks.

The reviewer says:

"While the material seems to be suitable to the scope of the journal, there are a number of points that I would like to see addressed before the paper is accepted."

I am unclear why they choose d_i as their measure of nonlinearity. They have not referenced where it has been used before, but I get the impression that it is not being introduced here."

Authors' response: We use a common measure of distance between time-series, and in the revised version we have included a sentence and relevant references.

The reviewer says:

"There are also a large number of techniques for measuring nonlinearity, so a comparison with established methods would also be helpful."

Authors' response: We agree with the reviewer and we remark that in the Supplementary Information we compare with an alternative measure and we obtain similar results (Fig. 2 in the SI).

The reviewer says:

"Additionally, nonlinearity in the atmosphere has been extensively studied, so a review of the pertinent material should be included in the introduction."

Authors' response: In the revised manuscript we have re-written the introduction and include a discussion of previous studies of nonlinearity in the atmosphere.

The reviewer says:

"I'm unsure why they believe the large time lag over the Amazon rainforest is due to the summer monsoon, and I would like them to more fully explain their reasoning."

Authors' response: As we say in the revised manuscript, the large lag in the Amazon rainforest does not have a straightforward explanation and we only speculate that a possible reason is due to the summer monsoon. We have modified the manuscript to explain why we consider this is a possible reason.

The reviewer says:

"The strong peak and low entropy values discussed are most likely a result of the binning procedure used, and a more thorough discussion of it is required."

Authors' response: We agree with the reviewer and in the revised manuscript we clarify this point. We have included this sentence: By normalizing each time series to zero mean and unit variance, we effectively adapt the range of values of SAT/SATA to the changing range of extreme values at different positions. While this might seem contradictory with performing "inter-site comparisons", this allows focusing the analysis in local extreme values (in other words, values that are extreme for the local SAT/SATA distribution).

The reviewer says:

"On L:10,11 They define $y_i(t)$ to be the SAT, and $x_i(t)$ to be the solar insolation. However, Eq.1 and their choice of lags suggest that they are searching for the effect of the SAT on the solar insolation at a later time? This does not seem reasonable, and I believe they have included the lag in the wrong term in Eq.1."

Authors' response: We agree with the reviewer and in the revised manuscript we corrected this mistake.

The reviewer says:

"As mentioned by other referees, the figures are improperly labelled and captioned, disagreeing with the text at some points. Isolation is frequently mistakenly used where insolation is meant."

Authors' response: We agree with the reviewer, we have carefully revised the manuscript and corrected these and other mistakes.

Identifying global patterns of stochasticity and nonlinearity in the Earth System

Fernando Arizmendi¹, Marcelo Barreiro¹, and Cristina Masoller²

¹Instituto de Física, Facultad de Ciencias, Universidad de la República, Iguá 4225, Montevideo, Uruguay

²Departament de Física, Universitat Politècnica de Catalunya, 08222 Terrassa, Barcelona, Spain

Correspondence to: F. Arizmendi (arizmendi.f@gmail.com)

Abstract. By comparing time-series of surface air temperature (SAT, monthly reanalysis data from NCEP CDAS1 and ERA Interim) with respect to the top-of-atmosphere incoming solar radiation (the insolation), we perform a detailed analysis of the SAT response to solar forcing. By computing the entropy of SAT time-series, we also quantify the degree of stochasticity. We find spatial coherent structures which are characterized by high stochasticity and nearly linear response to solar forcing (the shape of SAT time-series closely follows that of the insolation), or vice versa. The entropy analysis also allows to identify geographical regions in which there are significant differences between the NCEP CDAS1 and ERA Interim datasets, which are due to the presence of extreme values in one dataset but not in the other. Therefore, entropy maps are a valuable tool for anomaly detection and model inter-comparisons.

1 Introduction

The complex behavior of the atmosphere has attracted large interest in the last decades, as improving our understanding of its nature is important for advancing long term forecasts (e.g., Sugihara et al., 1999). Atmospheric nonlinearity has been studied using simplified models (Lorenz, 1963; Kondrashov et al., 2011), analyzing dynamical fields using statistical modal decomposition (Branstator and Berner, 2005) and Lyapunov exponents (e.g., Selten, 1993). Studies have shown that tropical and extratropical regions behave very differently as they respond to insolation in disparate manners. In the extratropics hydrodynamical instabilities dominate and the atmospheric behavior is highly nonlinear. For example, baroclinic instability is thought to be responsible for the development of cyclones, anticyclones and fronts, that is, the elements of day-to-day weather (Charney, 1947; Trenberth, 1991). These phenomena are very efficient in transporting heat from the tropics to the poles thus decreasing the equator-to-pole temperature gradient. Averaging over time scales longer than synoptic, it is thus expected for stochasticity to be large in the extratropics. In the tropics the excess of heat is transported to the extratropics through a thermally direct cell, the Hadley circulation. Moreover, on synoptic time scales, while tropical small scale and short-living phenomena are inherently nonlinear, such as convection and the development of mesoscale complexes, the large scale atmospheric variability is primarily linear in terms of waves that result from sea and land-surface forcing (Matsuno, 1966; Gill, 1980, 1982).

On the other hand, coupling between the different components of the climate system is strong in the tropical regions. Two well known examples are the monsoons and the ocean cold tongue dynamics. The monsoons are the result of the movement of

tropical convection due to seasonal changes in the land-sea temperature contrast and thus do not depend on the local insolation. These are regions where the large scale circulation, soil moisture and surface temperature interact strongly generating large climate variations. For example, monsoons have been shown to present nonlinear behavior on intraseasonal time scales (e.g., Chattopadhyay et al., 2008) as well as large interannual variability (e.g., Walker et al., 2015). Similarly, in the equatorial oceans, dynamical air-sea interactions are strong and have been shown to modify the sea surface temperature response to solar forcing. For example, while in the eastern equatorial Pacific the insolation presents two maxima as the sun crosses the Equator twice a year, the seasonal cycle of sea surface temperature has only one peak. Several authors have demonstrated that complex coupled atmosphere-ocean processes are responsible (e.g., Mitchell and Wallace, 1992; Chang and Philander, 1994). This has also consequences for the latitudinal movement of the Intertropical Convergence Zone: while over land the ITCZ tends to follow the sun, over the eastern basins the ITCZ are located almost year round to the north of the equator. Thus, these are all regions where a simple response to the direct solar forcing will not expected to be found.

The goal of this study is to perform a systematic study of nonlinearity and stochasticity in the atmosphere, which, to the best of our knowledge has not yet been done. We aim to answer the following questions: where are the global regions in which the response to solar forcing is strongly distorted due to local or nonlocal nonlinear processes and, which are the regions with largest stochasticity? Is there a relationship between these two quantities? To do so we will compare the local insolation with a measure of atmospheric response. We will analyze monthly mean surface air temperature (SAT) because it provides an integrated picture of the Earth system's reponse to insolation as it strongly depends not only on the direct solar forcing but also on the transport of heat due to atmospheric processes.

Besides providing a more complete picture of the nature of the atmospheric response to insolation, results may have consequences for the construction of climate networks. Climate networks, which are defined over a regular grid of geographical locations (nodes) covering the Earth surface, have proven to be a valuable analysis tool for understanding climate phenomena (Tsonis et al., 2006; Tsonis and Swanson, 2008; Yamasaki et al., 2008; Donges et al., 2009; Barreiro et al., 2011). In climate networks, a link between two nodes is defined in terms of a bivariate statistical similarity analysis of time-series of a climate variable (e.g., SAT) recorded at each node. However, similar response to solar forcing and/or similar stochastic properties of climate variability can lead to the identification of spurious links which do not represent actual interactions.

Finally, several studies have shown that the annual cycle of surface temperature has changed over the past 60 years toward earlier seasonal phasing and smaller amplitude over most land regions, but a delay in the phase over the ocean (Thomson, 1995; Mann and Park, 1996; Wallace and Osborn, 2002; Qian and Zhang, 2015). Mechanisms to explain these changes include loss of sea ice (Dwyer, 2012), large scale decreases in soil moisture which decrease the lag time between insolation and temperature by lowering the thermal inertia of the surface (Seager et al., 2007; Stine et al., 2009) and changes in shortwave optical properties that also alter the temperature lag behind insolation (Wallace and Osborn, 2002). Recently, Stine et al. (2012) proposed that changes in the northern extratropics can be related to variations in well known atmospheric circulation patterns. Thus, the separation between stochastic regions and those that respond nonlinearly to solar radiation may help in identifying areas that will be sensitive to antropogenic forcing given their complex response to insolation.

4 2 Datasets

We consider monthly mean SAT data from two reanalysis data sets: NCEP CDAS1 (Kalnay et al., 1996) and ERA Interim (ERA Interim, 2000). The spatial resolution is $2.5^\circ/1.5^\circ$ and cover the time-period [1949-2011]/[1979-2013] respectively. The NCEP CDAS1 reanalysis has $N = 10224$ SAT time-series of length $L = 756$ while in ERA Interim, $N = 28562$ of $L = 408$. The insolation at the top of the atmosphere is calculated following Berger (1978), as a function of day of year and latitude. Then, monthly averaged values for every latitude are calculated.

10 3 Methods of time-series analysis

To investigate the local response to solar forcing we compare SAT time-series in each grid point, $y_i(t)$, with the top-of-atmosphere incoming solar radiation (the insolation), in the same location, $x_i(t)$, assuming an adhoc, heuristic approach that there is a functional relation between them, $y_i = F(x_i)$. We are interesting in assessing the similarity of the shape of $x_i(t)$ and $y_i(t)$ time-series, which captures the nonlinear nature of the functional relation between them. Therefore, after normalizing the two time-series to have zero mean and unit variance, we calculate the difference between them **using a rectilinear distance, which is known as *taxicab* metric and has been used for example for analyzing urban problems and to assess differences in discrete frequency distributions (Krause, 1975; Lim et al., 2011),**

$$18 \quad d_i = \sum_{t=1}^L |x_i(t) - y_i(t + \tau_i)|. \quad (1)$$

Here τ_i is a shift that takes into account that there can be a lag-time between the two time-series, due, for example, to inertia and/or memory effects. This lag is expected to be important in the oceans in comparison with land masses, because of the larger heat capacity of water. Thus, at each location, i , the lag-time τ_i is calculated such as to minimize d_i . We search the minimum considering τ_i values in the interval [0,4] months because of the lack of physical mechanisms that could result in more than four months delay in SAT response with respect to the insolation forcing. **Sensitivity to maximum lags is shown in Supplementary Information, Fig. S1.**

Because we focus on the mean response to solar forcing, τ_i is calculated to minimize the distance between the insolation and the climatology (the averaged monthly SAT); similar results were found when considering the raw SAT time-series instead.

We note that, if the response is perfectly linear, after normalizing and computing the lag, we have $y_i(t + \tau_i) \sim x_i(t)$ and thus, $d_i \sim 0$. Therefore, by measuring how different in shape the two time-series are, d_i quantifies the distortion in the output response (SAT time-series) with respect to the input signal (the solar forcing represented by the insolation). It is worth to mention that, in Eq. (1), if instead of using $|x_i(t) - y_i(t + \tau_i)|$ we use $(x_i(t) - y_i(t + \tau_i))^2$, then d_i is equal to $2(1 - \rho_i)$ where ρ_i is the cross-correlation coefficient between $x_i(t)$ and $y_i(t + \tau_i)$ (see Fig. S2). **We note that more generic relations such as $y(t) = \int_0^t g(t - t')x(t')dt$ are also linear, however, here we only consider linear relationships involving only the present and only one past time.**

4 To quantify the stochasticity of the SAT time-series, we calculate the classical Shannon entropy, defined as

$$H_i = - \sum_n p_n \log p_n / H_{max} \quad (2)$$

6 where $p_i = \{p_n\}$ with $n = 1 \dots M$ and $\sum_n p_n = 1$ is the probability distribution associated to the SAT time-series $x_i(t)$,
and M is the number of bins. The entropy is normalized to the maximum value corresponding to the uniform distribution,
8 $H_{max} = \log M$. M is the same for all time-series within a reanalysis database, but is adjusted in each database to take into
account different length of the time-series: we consider 20 bins for ERA Interim and 40 bins for NCEP CDAS1. This gives an
10 **average of** the same number of data points per bin (~ 20). By normalizing each time series to zero mean and unit variance, we
effectively adapt the range of values of SAT/SATA to the changing range of extreme values at different positions. While this
12 might seem contradictory with performing "inter-site comparisons", this allows focusing the analysis in local extreme values
(in other words, values that are extreme for the local SAT/SATA distribution).

14 4 Results

Figure 1 presents the results of the forcing-response analysis. Figure 1(a) displays the map of d_i values computed without
16 shifting the insolation and SAT time-series, Fig. 1(b) displays the same but after shifting them a value $\tau_i \in [0, 4]$, and Fig. 1(c)
displays the map of τ_i values. These maps were obtained from the analysis of the ERA Interim dataset; similar results were
18 obtained from the NCEP CDAS1 dataset (see Fig. S3).

In Fig. 1(a) we observe large nonlinear responses in the tropics with coherent spatial structures over the oceans, with large
20 d_i values mainly in the cold tongues and areas associated with easterly trades and upwelling processes. Over the continents d_i
values are considerably smaller revealing a more linear insolation-SAT relation. There are exceptions, as in the Amazon and
22 the African rainforest, which show high d_i values.

When the time-series are shifted, Fig. 1(b), the largest d_i values appear over the tropical rainforests of Africa and South
24 America. These are the regions dominated by monsoons and can be expected because during the summer rainy season, when
the insolation has its highest values, the solar energy is used for evaporation instead of for heating. Moreover, as mentioned in
26 the introduction, the development of the monsoon depends on the land-sea contrast and not only on the local insolation.

In the oceans, also in the tropics, there are coherent spatial structures, with high d_i values on the equator, which tend to
28 coincide with regions of deep convection in the Atlantic, Pacific and Indian oceans, including the Intertropical Convergence
Zone (ITCZ). In these regions the SAT and rainfall are strongly coupled so that relatively small changes in SAT gradients
30 modulate and shift the ITCZ. In particular, air-sea coupling in the eastern basins induce oceanic cold tongues which together
with the continental geometry maintain warm waters and the ITCZ to the north of the equator (Philander et al., 1996) thus
32 introducing a nonlinearity in the SAT reponse. Outside the 10°S - 10°N band, the higher d_i values over the eastern subtropical
north Pacific, as compared to the western basin, can be due to the influence of the semi-permanent anticyclone and associated
2 stratus clouds. These clouds shield solar radiation and cool the sea surface, which in turn increases the static stability of
the atmosphere producing more stratus decks. This positive stratus-surface temperature feedback thus results in a nonlinear

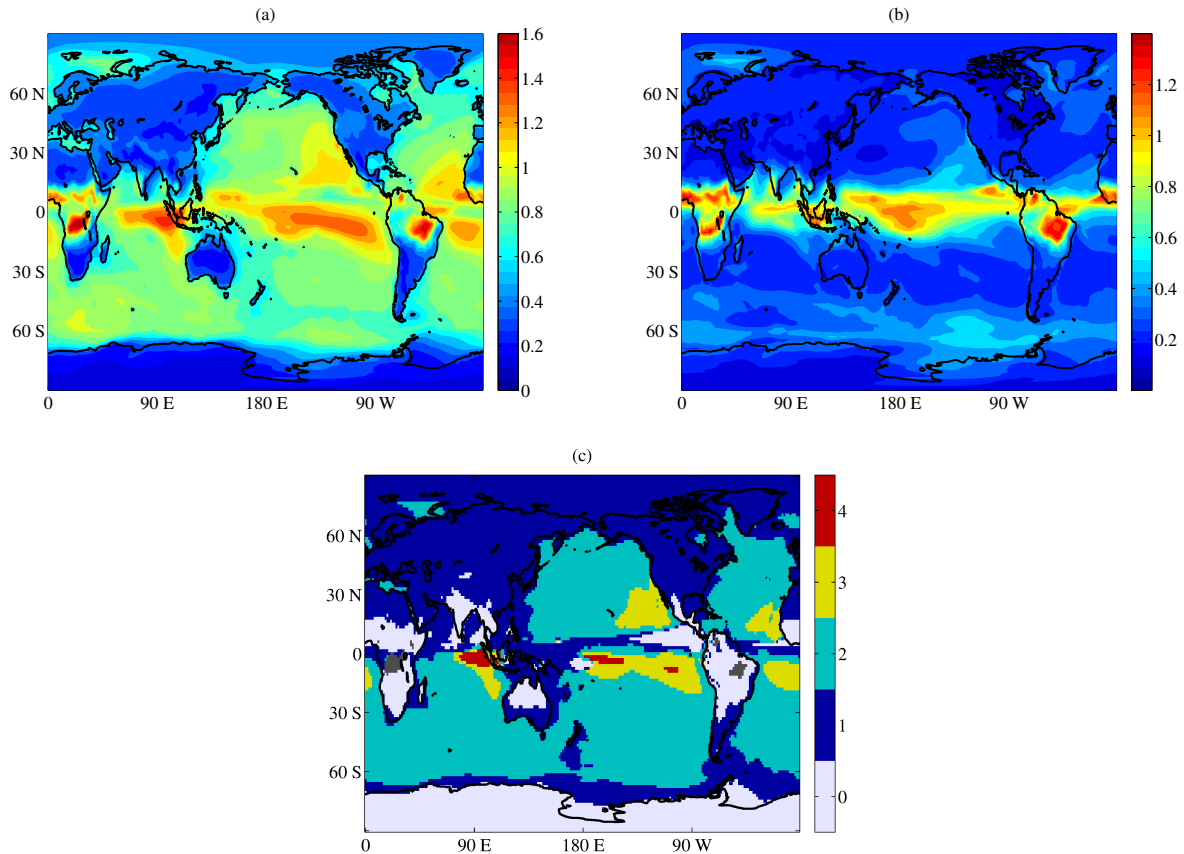


Figure 1. (a) Map of distances d_i calculated from Eq. (1) when the forcing (insolation) and the response (SAT) are not shifted ($\tau_i = 0$), (b) Map of distances, when the forcing and the response are shifted τ_i , with $\tau_i \in [0, 4]$. (c) Map of τ_i values. We exclude regions from Congo and Amazon rainforest (dark grey colored) where an increase of insolation is not necessarily an increase in SAT (see text). Data from ERA Interim reanalysis.

4 response to the insolation. High latitude oceans (southern Ocean, Labrador sea, Greenland sea) also show relatively large d_i values, which can be interpreted as due to the existence of seasonal sea ice in the regions.

6 The map of τ_i values, which is shown in Fig. 1(c), uncovers a rather symmetric behavior between both hemispheres. Overall, extratropical land masses have a lag of about 1 month, while extratropical oceans present a lag of 2 months, in agreement with
8 McKinnon et al. (2013). In tropical oceanic areas τ_i displays values in the [0-4] range, with values close to 0 and 1 in the ITCZ region and $\tau_i = 3$ in the eastern basins dominated by stratus clouds.

There are two continental regions, in the African tropical rainforest and in the Amazon rainforest that behave rather dif-
2 ferently. In these regions, the annual maximum of precipitation occurs during the summer monsoon, that is, precipitation is maximum at the time of maximum insolation.

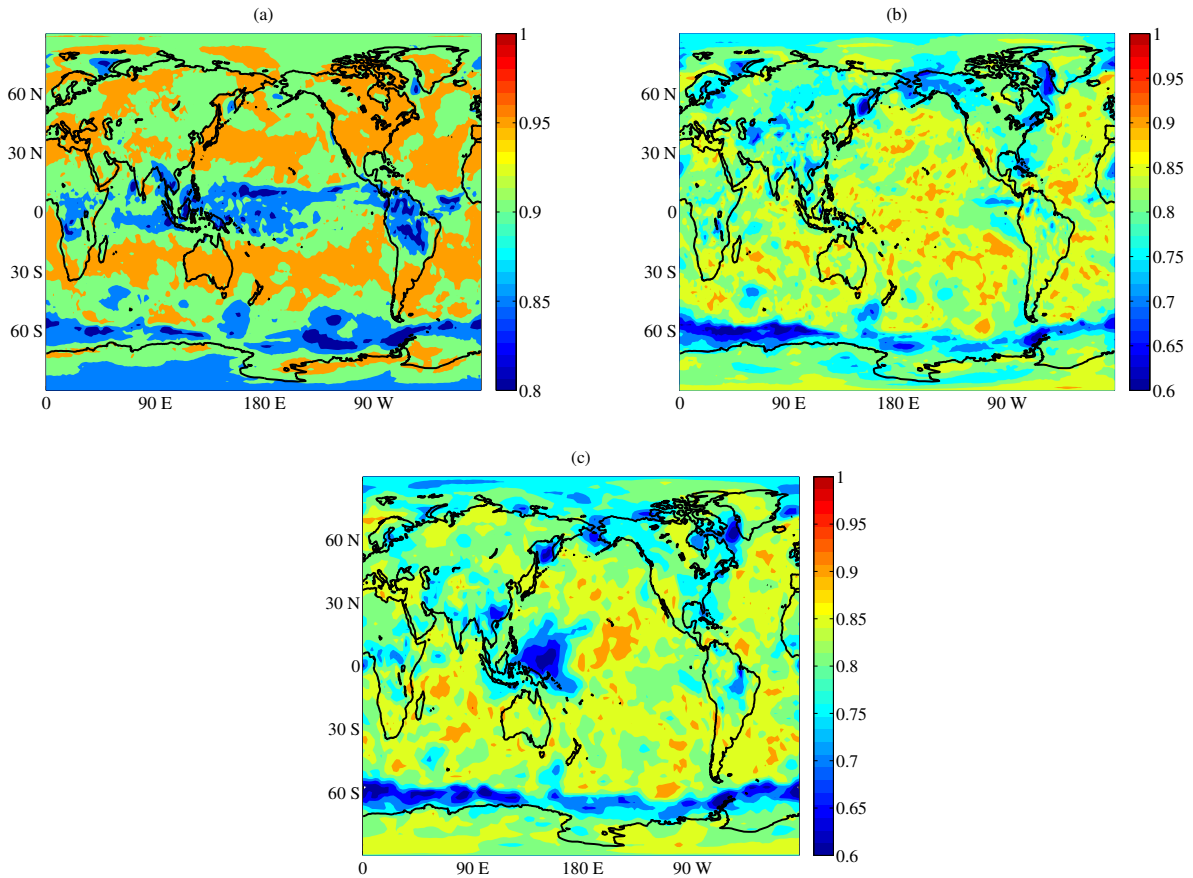


Figure 2. Map of Shannon entropy of SAT time-series (a) and of SAT anomalies (b) calculated from ERA Interim reanalysis. The spatial structures in panel (a) are similar to those observed in Fig. 1 (b). (c) Entropy of SAT anomalies calculated from NCEP CDAS1 reanalysis. Comparing panels (b) and (c), we note a well-defined region in the western Pacific where the two data sets display significant differences.

4 However, as solar energy is used for evaporation instead of heating of the surface, the SAT maximum is in spring at the
beginning of the monsoon season. Also, SAT variance is maximum in September because the beginning of the monsoon
6 changes from year to year. Thus, here a lag does not suggest a warming of the region due to the increased solar insolation, but
the fact that SAT becomes colder in the summer compared to the spring because of intense rainfall.

8 Figure 2 presents the analysis of the stochasticity of SAT variability. Figures 2(a) and 2(b) display the entropy, H_i , computed
from SAT time-series and SAT anomalies (i.e., removing the mean annual cycle from the time series) respectively, using ERA
10 Interim reanalysis.

The spatial patterns emerging in the ERA Interim SAT entropy map, Fig. 2(a), is in good agreement with the map of d_i
2 values displayed in Fig. 1(b), computed from the same reanalysis after shifting the SAT time-series. We note however overall
that the values are opposite: regions with high H_i have low d_i , and vice versa. To quantify and better visualize the relationship

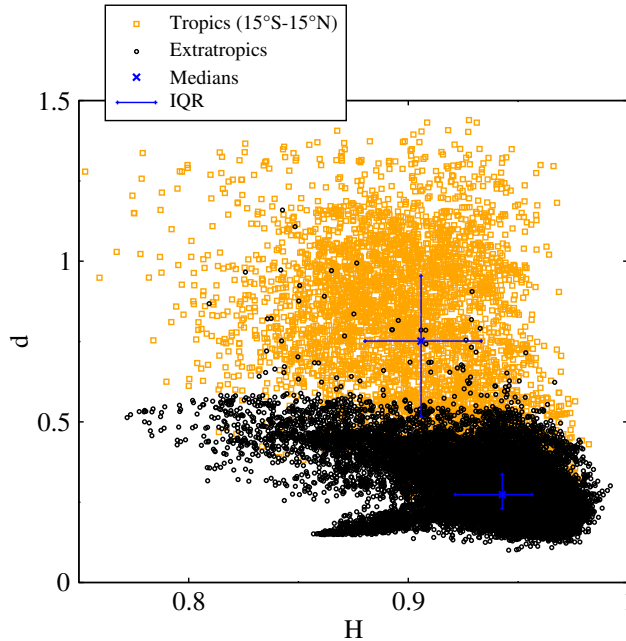


Figure 3. Entropy-distance map. The tropics (15°S - 15°N) and extratropics (90°S - 15°S , 15°N - 90°N) are represented in orange (squares) and black (circles), respectively. In addition, the blue crosses represent the respective medians with their correspondent interquartile ranges (blue lines).

- 4 between the entropy and the distance, in Fig. 3 there is a scatter plot of both quantities. The linear correlation between them is -0.45 . Tropical and extratropical regions have different characteristics in the d - H plane; as the interquartile range (IQR)
- 6 shows, tropics have larger d and smaller H , while extratropics have larger H and smaller d . Note that the distance used in this study allows for a clear separation between the two regions that is not as well captured by the entropy.
- 8 In addition, contrary to Fig. 2(a), in the entropy map of SAT anomalies displayed in Fig. 2(b) also for ERA Interim reanalysis, the main spatial patterns of the tropics seen in Fig. 2(a) disappear, and only those associated with sea ice remain. The latter
- 10 regions show a strong seasonality in their variance (that is not removed with the mean seasonal cycle) because while during summer the ocean heat fluxes control SAT, in winter the temperature can decrease considerably as the ice caps insulate the
- 12 atmosphere from the ocean. As result, the probability density functions show a long tail in low temperature values and entropy becomes small.
- 14 To check whether this is a robust result, we computed the entropy of SAT anomalies using NCEP CDAS 1 reanalysis (see also Fig. S4). The resulting map is presented in Fig. 2(c): it is very similar to that obtained from ERA Interim except in the western tropical Pacific where NCEP data shows minimum entropy. An inspection of SAT time-series in this region reveals the
- 2 existence of extreme values (outliers) which render the associated probability distribution to be peaked in a narrow interval, which in turn results in low entropy values. In ERA Interim there are also outliers, but, because they cover a very small area,

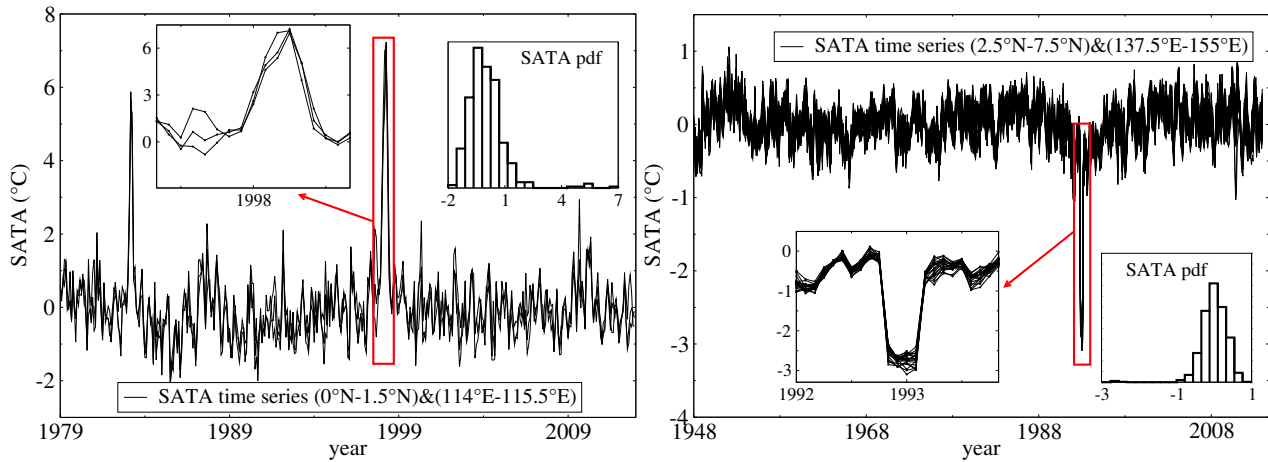


Figure 4. SAT anomaly time-series displaying extreme values in ERA Interim (*left*) and in NCEP CDAS1 reanalysis (*right*). The left (*right*) panel shows the time evolution of the 3 (21) grid points within the indicated domain.

4 their low entropy values cannot be seen in the entropy map shown in Fig. 2(b). Typical time-series of SAT anomalies in these regions, displaying extreme values, are presented in Fig. 4.

6 5 Conclusions

In this work we have investigated the stochastic properties of a climatological field (the surface air temperature, SAT) and its response to the solar annual forcing. We have characterized SAT stochasticity using Shannon entropy, and we have analyzed the response to solar forcing, by quantifying the similarity in the shape of the time-series of the top-of-atmosphere incoming solar radiation (the insolation) and the SAT, both having been previously normalized to have zero-mean and unit variance. The lag-time between the two time-series was taken into account by lagging the output response (SAT). Two reanalysis datasets were investigated, ERA Interim and NCEP CDAS1.

We found that the τ_i map in the extratropics is characterized by 1 month lag over the continental areas and 2 months lag over oceanic regions. In the tropical eastern ocean basins the lag increases to 3 months probably due to the presence of stratus clouds. The ITCZ region, on the other hand is mainly dominated by lags between 0 and 1 month. SAT over most tropical land areas show no lag with respect to the local insolation. There are, however, two particular regions in the Amazon and Congo basins that behave opposite from the rest of the world. These regions are characterized by strong monsoons and convection in which the SAT tends to cool in summer because the energy is used for evaporation instead of for surface heating. As result, maximum temperature is in spring, before the beginning of the monsoon.

After taking into consideration the lag, we found that the tropics show considerable nonlinear response to solar insolation. There are well-defined structures in the oceans, over the Intertropical Convergence Zones, and over some continental areas, especially in regions largely dominated by monsoons, such as the tropical rainforest in Africa and South America, as well as

4 over India. These regions do not respond to local insolation, but are characterized by strong air-sea coupling or land-atmosphere
interaction which involve non-local processes.

6 In the entropy maps we found very similar spatial structures, but with opposite values meaning that the geographical regions
with high d_i values correspond, in general, to regions with low entropy values, and vice versa. When the entropy was calculated
8 from the SAT anomalies, the tropical spatial patterns disappeared but those in the high latitudes remained. This was interpreted
as due to the fact that in high latitudes, mainly because of the presence of sea ice, there is a strong seasonality in variance that
10 remains even when the annual cycle is removed.

The entropy analysis also allowed to identify, in a well-defined region of the tropical western Pacific, a remarkable difference
12 between the ERA Interim and the NCEP CDAS1 data sets: in this region the datasets display extreme values, which cause the
pdf to be peaked in a narrow interval, resulting in low entropy values. Therefore, entropy maps can be used for anomaly
14 detection and model inter-comparisons.

Our results suggest that SAT over the tropical oceanic and continental regions (as well as those with sea ice) may be the
16 most sensitive to anthropogenic forcing because their evolution depend on a delicate coupling involving air-sea-land processes.
As future work, this could be addressed performing a similar analysis using the CMIP5 database to determine how the global
patterns identified here may change under an scenario of climate change.

2 *Acknowledgements.* This work was supported by the LINC project (FP7-PEOPLE-2011-ITN, Grant No. 289447). C. M. also acknowledges
partial support from Spanish MINECO (FIS2015-66503-C3-2-P) and ICREA ACADEMIA.

4 References

- Barreiro M., Martí, A. C., and Masoller, C.: *Chaos* **21**, 013101, 2011.
- 6 Berger, A.: *J. Atmos. Sci.* **35**, 2362, 1978.
- Branstator, G., and Berner, J.: *Journal of the atmospheric sciences*, 62(6), 1792-1811, 2005.
- 8 Chang P. and Philander, S. G.: *J. Atm. Res.* 51, 3627-3648, 1994.
- Charney, J. G.: *Journal of Meteorology*, 4(5), 136-162.
- 10 Chattopadhyay, R., Sahai, A. K. and Goswami, B. N.: *J. Atmos. Sci.*, 65, 1549-1569, 2008.
- Donges, J. F., Zou, Y., Marwan, N., and Kurths, J.: *Eur. Phys. J. Spec. Top.* **174**, 157, 2009.
- 12 Dwyer, J. G., Biasutti, M., and Sobel, A. H.: *Journal of Climate*, 25(18), 6359-6374, 2012.
- European Centre For Medium-Range Weather Forecasts (ECMWF). Shinfield Park, Reading, RG2 9AX, United Kingdom.
- 14 Gill, A.: *Quarterly Journal of the Royal Meteorological Society*, 106(449), 447-462, 1980.
- Gill, A. E.: *Atmosphere-ocean dynamics* (Vol. 30). Academic press, 1982.
- 16 Kalnay, E., et al.: *Bull. Amer. Meteorolog. Soc.* **77**, 437, 1996.
- Kondrashov, D., Kravtsov, S., and Ghil, M.: *Journal of the Atmospheric Sciences*, 68(1), 3-12, 2011.
- 18 Krause, E. F.: *Taxicab Geometry: An Adventure in Non-Euclidean Geometry*. Courier Corporation, 1975.
- Lim, K. H., Ferraris, L., Filloux, M. E., Raphael, B. J., and Fairbrother, W. G.: *PNAS*, 108(27), 11093-11098, 2011.
- 20 E. N. Lorenz, *J. Atmos. Sci.* **20**, 130 (1963).
- McKinnon, K. A., Stine, A. R., and Huybers, P.: *J. Climate* **26**, 7852, 2013.
- 22 Mann, M. E., and Park, J.: *Geophysical Research Letters*, 23(10), 1111-1114, 1996.
- Mitchell, T. P., and Wallace, J. M.: *J. Climate* **5**, 1140 (1992).
- 24 Matsuno, T.: *J. Meteor. Soc. Japan*, 44(1), 25-43, 1966.
- Philander, S. G., Gu, D., Halpern, D., Lambert, G., Ngar-Cheung Lau, Li, T., and Pacanowski, R. C.: *J. Climate*, **9**(12), 2958-2972, 1996.
- 26 Qian, C., and Zhang, X.: *Journal of Climate*, 28(15), 5908-5921, 2015.
- Seager, R., Ting, M., Held, I., Kushnir, Y., Lu, J., Vecchi, G., ... , and Li, C.: *Science*, 316(5828), 1181-1184, 2007.
- 28 Selten, F. M.: *Journal of the atmospheric sciences*, 50(6), 861-877, 1993.
- Stine, A. R., and Huybers, P., and I. Y. Fung: *Nature*, 457, 435-440, doi:10.1038/nature07675. 2009.
- 30 Stine, A. R., and Huybers, P.: *J. Climate*, 25, 7362-7380, doi:10.1175/JCLI-D-11-00470.1. 2012.
- Sugihara, G., Casdagli, M., Habjan, E., Hess, D., Dixon, P., and Holland, G.: *PNAS* **96** (25) 14210-14215; doi:10.1073/pnas.96.25.14210
- 32 Thomson, D. J.: *Science*, 268(5207), 59-68, 1995.
- Trenberth, K. E.: *J. Atmos. Sci.*, 48, 2159-2178, 1991.
- 34 Tsonis, A. A., and Swanson, K. L., *PRL* 100, 228502, 2008.
- Tsonis, A. A., Swanson, K. L. and Roebber, P. J: *Bull. Am. Meteorol. Soc.* **87**, 585, 2006.
- Wallace, C., and Osborn, T.: *Climate Res.*, 22, 1-11, 2002.
- 224 Walker, J. M., Bordoni, S. and Schneider, T.: *Journal of Climate*, 28(9), 3731-3750, 2015.
- Yamasaki, K., Gozolchiani, A., and Havlin, S.: *PRL*, **100**(22), 228501, 2008.